ELSEVIER

Precambrian Research 120 (2003) 219–239

Precambrian Research

www.elsevier.com/locate/precamres

Timing of deformation in the Norseman-Wiluna Belt, Yilgarn Craton, Western Australia

Roberto F. Weinberg [a,*], Louis Moresi [b], Peter van der Borgh [a]

[a] Centre for Global Metallogeny, Department of Geology and Geophysics, University of Western Australia, Nedlands, WA 6907, Australia
[b] DEM, CSIRO, Nedlands, WA, Australia

Received 10 December 2001; accepted 28 August 2002

Abstract

Establishing relative and absolute time frameworks for the sedimentary, magmatic, tectonic and gold mineralisation events in the Norseman-Wiluna Belt of the Archean Yilgarn Craton of Western Australia, has long been the main aim of research efforts. Recently published constraints on the timing of sedimentation and absolute granite ages have emphasized the shortcomings of the established rationale used for interpreting the timing of deformation events. In this paper the assumptions underlying this rationale are scrutinized, and it is shown that they are the source of significant misinterpretations. A revised time chart for the deformation events of the belt is established. The first shortening phase to affect the belt, D_1, was preceded by an extensional event D_{1e} and accompanied by a change from volcanic-dominated to plutonic-dominated magmatism at approximately 2685–2675 Ma. Later extension (D_{2e}) controlled deposition of the ca 2655 Ma Kurrawang Sequence and was followed by D_2, a major shortening event, which folded this sequence. D_2 must therefore have started after 2655 Ma—at least 20 Ma later than previously thought and after the voluminous 2670–2655 Ma high-Ca granite intrusion. Younger transcurrent deformation, D_3–D_4, waned at around 2630 Ma, suggesting that the crustal shortening deformation cycle D_2–D_4 lasted approximately 20–30 Ma, contemporaneous with low-volume 2650–2630 Ma low-Ca granites and alkaline intrusions. Time constraints on gold deposits suggest a late mineralisation event between 2640–2630 Ma. Thus, D_2–D_4 deformation cycle and late felsic magmatism define a 20–30 Ma long tectonothermal event, which culminated with gold mineralisation. The finding that D_2 folding took place after voluminous high-Ca granite intrusion led to research into the role of competent bodies during folding by means of numerical models. Results suggest that buoyancy-driven doming of pre-tectonic competent bodies trigger growth of antiforms, whereas non-buoyant, competent granite bodies trigger growth of synforms. The conspicuous presence of pre-folding granites in the cores of anticlines may be a result from active buoyancy doming during folding.

Keywords: Kalgoorlie orogen; Gold mineralization; Archean tectonics; Extension; Granite doming; Buoyancy

1. Introduction

On the eastern part of the Archaean Yilgarn Craton, the Eastern Goldfields Province is composed of several belts trending approximately

* Corresponding author
E-mail address: rweinber@geol.uwa.edu.au (R.F. Weinberg).

0301-9268/02/$ - see front matter
PII: S0301-9268(02)00142-0

NNW-SSE. Gee (1979) identified the Norseman-Wiluna Belt as the major component of the western part of the Eastern Goldfields Province (Fig. 1). Barley et al. (1989) subdivided the belt into an eastern sequence typical of modern volcanic arcs, and a western sequence comparable to submarine marginal or back-arc basins. Two main periods of volcanism have been recognized in the Norseman-Wiluna Belt (e.g. Campbell and Hill, 1988): the older, >2900 Ma, is sparsely exposed and is overlain by a younger ~ 2700 Ma succession of greenstones surrounded, and intruded, by granitic rocks. This paper is concerned with the timing of structural events which deformed the younger succession.

Structural research in orogenic belts is aimed at devising models for their tectonic evolution and predicting the 3D geometry of the system. A well-constrained model for the structural evolution of a province provides immense predictive capacity, particularly when targeting structurally controlled mineral deposits. A common practice used for timing deformation events is to determine the relative age between structures and granite intrusions of known absolute age. For accurate results, however, it is essential that the relative timing between granite crystallization and deformation be uniquely constrained by field observations and detailed micro structural studies. This is particularly relevant for the Yilgarn Craton where granite bodies are considered to have played a major role on its structural evolution. This paper explores the established views of the relationships between granite intrusion and deformation in the Norseman-Wiluna Belt, and demonstrates that these views are flawed and have led to significant misinterpretation of the tectonic evolution of the belt. The approach taken here is to use present understanding of the deformation phases that account for the structural evolution of the belt as a framework to understand their timing. It is beyond the scope of this paper to question the deformation phases themselves.

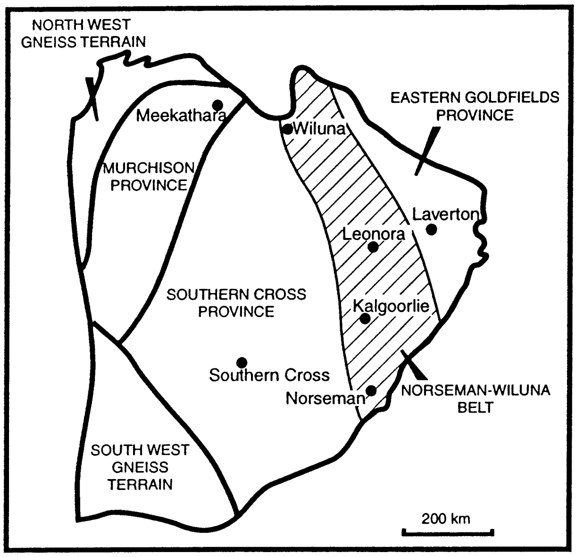

Fig. 1. Regional Map of the Archaean Yilgarn Craton delineating the provinces and the Norseman-Wiluna Belt (redrawn from Gee, 1979).

2. Regional deformation

A generally accepted deformation scheme for the Norseman-Wiluna Belt divides deformation into four main shortening phases, D_1–D_4 (e.g. Archibald et al., 1978; Platt et al., 1978; Witt and Swager, 1989; Swager et al., 1992; Swager 1997). D_1 is sometimes described as an extensional phase of isoclinal recumbent folding and sub-horizontal nappe-type translation (Archibald et al., 1978; Martyn, 1987; Passchier, 1994). Commonly, mostly in the southern part of the province, D_1 is described as a shortening phase associated with major thrusting (Martyn, 1987; Vearncombe et al., 1989; Witt and Swager, 1989; Swager and Griffin, 1990; Swager et al., 1992; Knight et al., 1993). D_1 movement direction is thought to be from south to north (Swager and Griffin, 1990). Swager (1997) interpreted the Bulong Anticline, east of Kalgoorlie, as a D_2 structure which folds a regional D_1 thrust. In this area, a 2705 ± 4 Ma komatiite–tholeiite assemblage was thrusted on top of a 2672 ± 12 Ma dacite (for ages see Nelson, 1997), presumably from the west (Swager, 1997). The maximum age of this D_1 structure is therefore 2684 Ma (corresponding to the maximum possible age of the dacite).

D_2 shortening structures overprinted D_1 structures and produced regional NNW–SSE trending, gently plunging folds associated with a steep foliation, S_2, that can be traced over long distances (Archibald et al., 1978; Platt et al., 1978; Witt and Swager, 1989; Swager and Griffin, 1990). D_3 was a transpressive event which overprinted D_2 and is associated with shear zones, usually sinistral, and en-echelon folds (Witt and Swager, 1989; Swager and Griffin, 1990). Initial foliation development occurred during F_2 folding and intensified during D_3. For the Kalgoorlie area, Swager et al. (1992) suggested gradual transition from D_2 to D_3 sinistral strike slip producing a single fabric. Near Leonora, Passchier (1994) found that D_2 and D_3 are effectively inseparable and suggested that there could have been a vorticity partitioning during the same event.

D_4 is a phase of continued regional shortening leading to dextral NNE–SSW trending shear and fault zones described for areas such as the Golden Mile and Mt. Charlotte mining areas (Mueller et al., 1988; Ridley and Mengler, 2000) and well-defined in a broader area to the north and west of Kalgoorlie. Mueller et al. (1988) mapped a number of fault sets, which they ascribed to a single phase of NNW–SSE dextral wrenching event, which cross-cut earlier NNW–SSE trending D_3 sinistral shear zones. Dextral shearing had previously been described on N–S and NNE–SSW trending shear zones (e.g. Platt et al., 1978; Passchier, 1994), but they have been considered to be part of D_3 by Hammond and Nisbet (1992). The nature and timing of dextral shearing throughout the belt remains ambiguous, but as well exemplified by the work of Ridley and Mengler (2000) in Kalgoorlie, the distinguishing feature of D_4 faults is their brittle and late character, compared to older ductile D_3 shear zones. D_4 will not be dealt with in any detail throughout the rest of the paper. Structurally controlled gold mineralisation is typically tectonically late, and mineralisation in a number of deposits is constrained by geochronology studies to have taken place between 2640 and 2630 Ma (Fig. 2; e.g. Groves et al., 1995, 2000).

Groves and Batt (1984) and Hallberg (1986) emphasised the importance of early extension in the evolution of the belt. However, extensional phases are less well-defined than shortening phases. The difficulty lies partly in the overprinting by shortening structures, and partly in separating a regional phase of extension from local extensional structures developed during regional shortening events. For example, Swager and Nelson (1997) suggested that the extensional structures around the Eastern Gneiss Complex are due to doming during shortening, whereas Passchier (1994) interpreted the early extensional structures around the Raeside granite near Leonora to be a result of regional extension, unrelated to doming. Hammond and Nisbet (1992) determined movement direction on a number of shear zones and concluded that the earliest set of ductile shears records an extensional event, which Williams and Whitaker (1993) argued was contemporaneous with an early phase of gneiss and granite doming. There is general consensus that there was an extension phase before D_1, which Hammond and Nisbet (1992) labelled D_e (Swager, 1997). Williams and Currie (1993), based on the N–S trend of early granite domes, suggested an east–west extension axis for this phase.

Witt (1994) inferred an extensional collapse stage following D_1 thrust stacking. The results of a regional east–west, deep crustal seismic reflection profile north of Kalgoorlie have indicated the presence of a prominent sub-horizontal reflector interpreted as a detachment underlying the greenstone sequence (Drummond et al., 1993; Goleby et al., 1993). Goleby et al. (1993) and Williams and Currie (1993) suggested that major east–west extension above the detachment resulted in truncation of greenstones and thrusts. This extension was interpreted to have taken place after D_1 thrusting but before D_2 shortening (Swager, 1997). According to Swager (1997) this extension accounts for the clastic deposits in basins folded during D_2, such as the Kurrawang Sequence, at the core of the Kurrawang Syncline, and the Merougil Sequence. He estimated extension to have occurred at approximately 2675 Ma. This contrasts with the recent results of Krapez et al. (2000).

Krapez et al. (2000) studied the timing of deposition of a number of volcano-sedimentary sequences in the Norseman-Wiluna Belt and found a number of unconformities, indicating phases of uplift and erosion (shortening?), separating phases

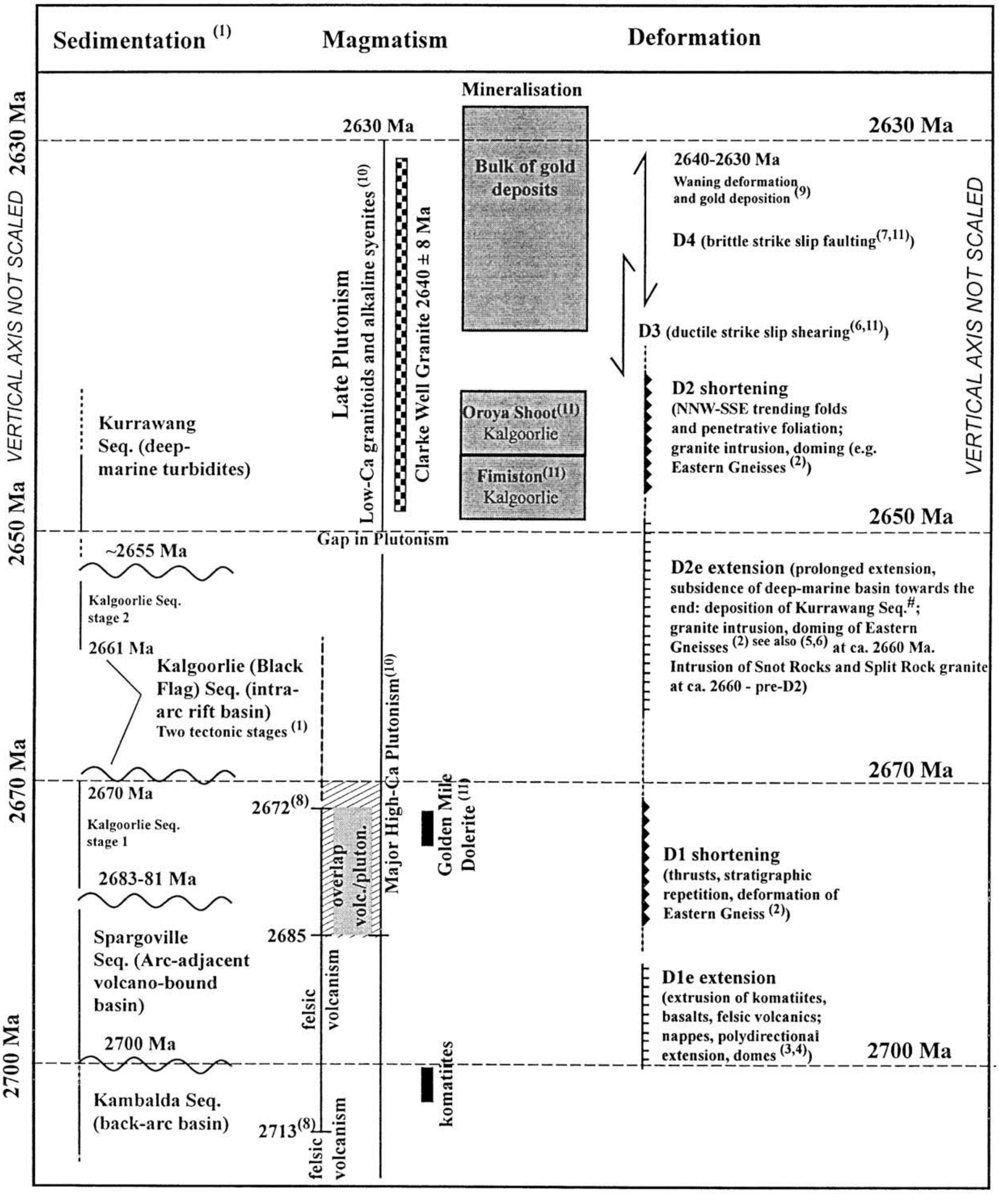
Sedimentation (1)
Magmatism
Deformation
Mineralisation
2630 Ma
2630 Ma
2630 Ma
VERTICAL AXIS NOT SCALED
Bulk of gold deposits
Late Plutonism
Low-Ca granitoids and alkaline syenites (10)
Clarke Well Granite 2640 ± 8 Ma
2640-2630 Ma
Waning deformation and gold deposition (9)
D4 (brittle strike slip faulting(7,11))
D3 (ductile strike slip shearing(6,11))
D2 shortening
(NNW-SSE trending folds and penetrative foliation; granite intrusion, doming (e.g. Eastern Gneisses (2))
Kurrawang Seq. (deep-marine turbidites)
Oroya Shoot(11) Kalgoorlie
Fimiston(11) Kalgoorlie
2650 Ma
2650 Ma
Gap in Plutonism
~2655 Ma
Kalgoorlie Seq. stage 2
2661 Ma
Kalgoorlie (Black Flag) Seq. (intra-arc rift basin)
Two tectonic stages (1)
D2e extension (prolonged extension, subsidence of deep-marine basin towards the end: deposition of Kurrawang Seq.#; granite intrusion, doming of Eastern Gneisses (2) see also (5,6) at ca. 2660 Ma. Intrusion of Snot Rocks and Split Rock granite at ca. 2660 - pre-D2)
Major High-Ca Plutonism(10)
2670 Ma
2670 Ma
2670 Ma
2672(8)
Kalgoorlie Seq. stage 1
overlap volc./pluton.
Golden Mile Dolerite (11)
D1 shortening
(thrusts, stratigraphic repetition, deformation of Eastern Gneiss (2))
2683-81 Ma
Spargoville Seq. (Arc-adjacent volcano-bound basin)
2685
felsic volcanism
D1e extension
(extrusion of komatiites, basalts, felsic volcanics; nappes, polydirectional extension, domes (3,4))
2700 Ma
2700 Ma
2700 Ma
komatiites
Kambalda Seq. (back-arc basin)
2713(8)
felsic volcanism

Fig. 2.

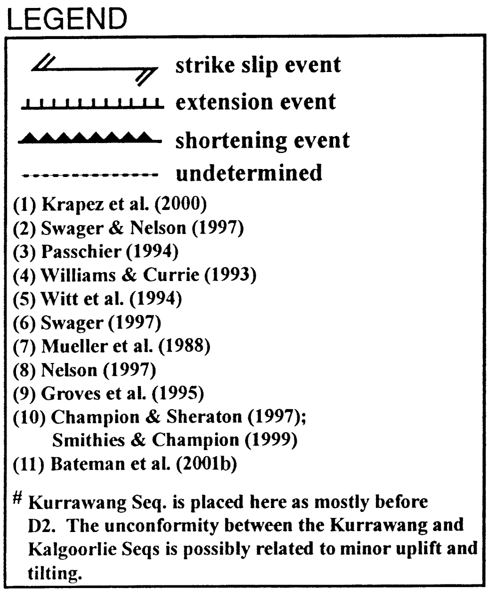

Fig. 2. Time chart summarizing sedimentation, magmatism and deformation of the Norseman-Wiluna Belt. Note that the vertical axis, corresponding to time evolution is not scaled for the sake of clarity. In contrast to previous interpretations, D_2–D_4 are all post-2655 Ma, since D_2 must have occurred after the initiation of sedimentation of the Kurrawang Sequence. This implies that the voluminous high-Ca granite bodies were emplaced before D_2–D_4 transcurrent events.

of subsidence. They found that the Kurrawang Sequence comprises a succession of quartzofeldspathic conglomerate, sandstone and mudrock representing high-density–low-density turbidites, deposited in a deep-marine environment. An erosional unconformity separates the Kurrawang Sequence from the underlying Kalgoorlie Sequence (formerly Black Flag Group). The deposition of the Kalgoorlie Sequence is divided into two tectonic stages with depositional ages between 2681–2670 Ma and 2661–2655 Ma (Fig. 2), as constrained by zircon ages (Krapez et al., 2000). These ages and the unconformity imply sub-aerial uplift and erosion of the Kalgoorlie Sequence followed by rapid drowning and deposition of the Kurrawang Sequence after 2655 Ma (Krapez et al., 2000). The deposition of the Kurrawang Sequence requires an important phase of subsidence after D_1. The late deposition of the Kalgoorlie and Kurrawang Sequences implies that earlier interpretations of the timing of deformation based on their early deposition must be reassessed.

The new results of Krapez et al. (2000) demand a careful scrutiny of the assumptions behind the established view of the timing of deformation. It is the purpose of this paper to discuss the limitations of these assumptions, and to propose alternative interpretations and a new time chart for the structural evolution of the Norseman-Wiluna Belt. This paper starts with a short description of the established view of the structural evolution of the belt. The shortcomings of the assumptions underlying this view are then demonstrated, while a new time chart for the structural events is erected. Because granite plutons are such an essential part of this problem, the results of numerical models illustrating the role of competent granites during folding are described.

3. Relative timing of granite intrusion: the established view

A large number of crystallization ages of felsic magmatic rocks of the Yilgarn Craton have been determined over the last decade (e.g. Nelson, 1997; Brown et al., 2001). Many granite gneisses previously interpreted as basement rocks have now been shown to be intrusive into the greenstone sequence (e.g. Swager and Nelson, 1997). It has also been found that early granite intrusions in the Norseman-Wiluna Belt are contemporaneous with the youngest felsic volcanic rocks and were intruded at approximately 2685–2675 Ma (e.g. Campbell and Hill, 1988; Nelson, 1997). The most voluminous intrusion event occurred between 2675 and 2655 Ma (Nelson, 1997). These absolute ages were used to constrain the timing of deformation by using Witt and Swager's (1989) tectonic/structural classification of granites of the Ora Banda-Coolgardie area (NNW and W of Kalgoorlie, respectively) (Table 1; e.g. Swager et al., 1992; Nelson, 1997; Witt and Davy, 1997).

Witt and Swager (1989) defined a pre- to syn-D_2 group of granites characterized by ellipsoidal shapes at the cores of regional F_2 anticlines. These were followed by post-D_2 syn-D_3 granites, which form ovoid to circular bodies and display a well-defined, contact parallel foliation. They occur as individual plutons or in clusters, where single plutons are separated by narrow screens of poorly exposed greenstones (traced by their distinct aeromagnetic expression). In Witt and Swager's (1989) view, these plutons either pushed aside F_2 regional upright folds or were emplaced across them. They used the displaced axial trace of the Kurrawang Syncline in the vicinity of granites in the Siberia area as an example. Another example is the Bali monzogranite, which was interpreted to displace and cross-cut an F_2 anticline (Witt and Swager, 1989).

Several of these granites appear to be bounded by regional D_3 shear zones. Unlike F_2 folds, these shear zones are not deflected to any large extent by the granites and overprint contact foliation, indicating that D_3 transcurrent faulting at least partly post-dated emplacement of these granites (Witt and Swager, 1989). Late-tectonic plutons (late- to post-D_3) are unfoliated or only weakly sheared by D_3 shear zones and generally have ages equal to or smaller than 2640 Ma (Campbell and Hill, 1988; Nelson, 1997).

3.1. Assumptions

In order to understand the timing relationship between granite emplacement and structural evolution of the belt, and the origin of the discrepancies in the literature, it is necessary to fully explore the assumptions underlying Witt and Swager's (1989) rationale. These are: (a) the degree of deformation of granites is related to the time of magma crystallization in relation to the time of deformation, e.g. weakly sheared granites are late-tectonic; (b) pre- or syn-D_2 granites lie at the core of anticlines; and (c) granite emplacement causes deviation of structures (e.g. folds) from their regional trend, i.e. granite post-dates structures. A fourth, more general assumption, often made implicitly, is that: (d) the age of magma crystallization, as derived from SHRIMP zircon dating, represents the age of granite emplacement. This assumption neglects the possibility that final emplacement geometry of large granite bodies may have taken place in the solid state as diapirs or core complexes.

These assumptions are not necessarily incorrect, their problem is that they do not uniquely define the timing of granite intrusion in relation to deformation. Their use, implicit or explicit, lies at the core of the discrepancies between absolute age of granites and their interpreted structural context.

4. Strain intensity and granite age

The use of granite strain intensity to estimate the relative timing of granite intrusion—assumption (a)—is deeply rooted in the geological literature, despite numerous contributions outlining its pitfalls (e.g. Archibald et al., 1978; Paterson and Tobisch, 1988). In the Yilgarn, early classification of granites was based on a combination of strain intensity and other structural characteristics (Archibald and Bettenay, 1977), and has since permeated the literature. Champion and Sheraton (1997) avoided these pitfalls by developing a geochemical classification for granite intrusions of the Leonora-Lenster area (Norseman-Wiluna Belt).

Table 1
Structural evolution and timing of granite intrusion: the established and new views

Deformation phases[a]	Granite intrusion[b]	This work
	Late- to post-tectonic low-Ca granites: 2650-2630 Ma. Equidimens., relatively small, unfoliated. Include alkaline igneous rocks (Smithies and Champion 1999)	
D_4 dextral shearing on NNE–SSW trending zones (Mueller et al., 1988; Ridley and Mengler, 2000)		D_4 brittle dextral shearing. Low-Ca granitoid intrusion throughout D_2–D_4
D_3 strike slip shear zones with both sinistral and dextral movement. Approximately 2663–2632 Ma.	Post- D_2 syn- D_3 granites, deflect D_2 folds and are cut by D_3 shear zones	D_3 sinistral and dextral (conjugate) shearing waning at 2630 Ma. Contemporaneous to and outlasting D_2
D_2 upright folds, associated axial planar fabrics reflecting penetrative ENE-WSW shortening. Local extension around granite domes. Approximately 2675–2657 Ma.	Pre- to syn- D_2 granites in cores of anticlines	D_2 shortening, syn- or late-deposition of the Kurrawang Seq. (2655 Ma). Folding and doming of granite bodies driven by interaction granite buoyancy-regional stresses
D_{2e} (Witt, 1994; Swager, 1997) east–west extension (Goleby et al., 1993)		D_{2e} follows D_1 at <2672 to >2655 Ma, pre-dates Kurrawang Seq. Doming of Eastern Gneiss Complex and intrusion of voluminous high-Ca granites
D_1 low angle shear zones, thrusts and stratigraphic repetition, 2675 Ma (Swager and Nelson 1997)		D_1 shortening starts at approximately 2683 Ma, active to <2672 Ma. Unconformity between Spargoville Seq. and Kalgoorlie Seq.? (Krapez et al., 2000)
		Overlap between felsic volcanism and plutonism. Instrusion of 2675 Ma Eastern Gneissic Complex
D_e low-angle shear zones along granite-greenstone contacts, top-to-SSE movement sense, polydirectional extension (Hammond and Nisbet 1992; Passchier, 1994)		D_{1e}

[a] Compiled after Swager (1997), Witt and Swager (1989), Nelson (1997) and Ridley and Mengler (2000).
[b] After Witt and Swager (1989) and Smithies and Champion (1999).

The strain intensity recorded by granites depends on a range of factors. Apart from the timing of intrusion, strain intensity depends also on deformation related to magma pressures (Paterson and Tobisch, 1988; Weinberg and Podladchikov, 1995), on the shape and size of the granite body, on the depth of emplacement, on the location of the granite in relation to pre-existing high strain zones, as well as on the competence contrast to the country rocks. With the exception of coarse-grained pegmatites, narrow bodies such as granite dykes are relatively easily deformed. Large, ellipsoidal granite plutons, surrounded by relatively incompetent rocks such as phyllosilicate-dominated rocks (Robin, 1979; Wintsch et al., 1995) will behave rigidly and deflect deformation rather than record it. By contrast a similar pluton, at high-temperature and surrounded by relatively competent amphibolites, may behave incompetently. Furthermore, a cooling granite body may change from relatively incompetent to competent.

In the Norseman-Wiluna Belt, shear strain is partitioned to well-defined deformation corridors (e.g. the Bardoc and Zuleika-Kunanalling Shear Zones in Fig. 2 of Witt and Swager, 1989) composed predominantly of phyllosilicate-rich green schist facies rocks. These corridors deflect around large masses of granite giving rise to large-scale lozenges suggesting organization of deformation into corridors around competent granite cores.

The difficulty in relating strain intensity to time of magma intrusion is best exemplified in the Yilgarn by the Siberia Battery syenogranite. This body was interpreted by Witt and Swager (1989) as being post-D_3 because it is only weakly deformed where cut by D_3 shear zones. However, recent dating yielded a crystallization age of 2673 ± 3 Ma for the syenogranite (Nelson, 1997, sample 98 256), making it contemporaneous to complexly deformed gneisses interpreted to be pre-D_2, such as the foliated Two Lids Soak granodiorite and the Barret Well orthogneiss (Nelson, 1997, samples 112 153 and 112 179, respectively). The differences in strain intensity could be simply due to emplacement depth or strain-rate partitioning across the belt (Davis et al., 2001).

Another example is the weakly deformed 2640 ± 8 Ma old Clarke Well monzogranite, which cross-cuts the Ida Fault, the western boundary of the Norseman-Wiluna Belt. It was used to constrain the minimum age of D_3 movement on the fault (Nelson, 1997), but just as the granite may have intruded after D_3, it may have intruded an inactive part of a wide fault zone.

5. Folding and deflection: timing of D_2

Assumption (b) above, that granites in the core of F_2 anticlines are pre- to syn-D_2, and (c), that deflection of regional trends is caused by granite emplacement, are both flawed. Whether or not granites lie at the core of folds depends on the timing of deformation as well as on the mechanism of granite emplacement (Paterson and Tobisch, 1988). Pre-tectonic rigid granites can control the sites of synclinal and anticlinal folds. Diapirically emplaced granites may cause the development of anticlines (as in the numerical models below), conversely granitic melt will tend to migrate to fold hinge zones of pre-existing fold hinges or growing antiforms (Allibone and Norris, 1992; Davis, 1993; Weinberg, 1996).

The role of pre-existing granites during folding depends on the competence contrast to the country rocks and on the characteristic wavelength of the folds. Granites in the Norseman-Wiluna Belt have responded to deformation mainly as competent bodies. This is evidenced by shearing and shortening of the greenstones and granite-greenstone contacts while granite away from pluton margins remain weakly deformed. Granite dykes are also commonly boudinaged, and importantly, regional structures are deflected around elliptical granite bodies, similar to the deflection of foliation around rigid porphyroblasts.

A narrow competent granite body will commonly fold together with the entire package, while a wide competent granite will act as a buttress while folds develop in their country rocks. These folds wrap around the rigid body as a result of regional deformation and not as a result of magma emplacement efforts. Thus, contrary to assumption (c), early emplaced granites may cause deflection of structures developed long after granite emplacement, (see also Paterson and Tobisch, 1988). The role of granite bodies of sizes comparable to typical fold wavelengths of a rock sequence is explored below (Section 8).

An illustrative example of the problems related to assumption (c) is the deflection of the F_2 Kurrawang Syncline, which includes the Kurrawang Sequence, from its NNW–SSE regional trend. Witt and Swager (1989) estimated a deflection of approximately 15 km, as it approaches the 2660 ± 3 Ma Snot Rocks monzogranite (Nelson, 1997). Deflection was interpreted to have resulted from granite intrusion, implying that the intrusion post-dated deposition of the Kurrawang Sequence and F_2 folding (Witt and Swager, 1989; Nelson, 1997). By contrast, the Split Rock granodiorite, which crops out at the core of the Scotia-Kanowna Dome, a regional F_2 anticline 40 km SE of the Snot Rocks, was interpreted by Witt and Swager (1989) to be pre- to syn-D_2. However, when dated, the granodiorite yielded a crystallization age of 2657 ± 5 Ma (Nelson, 1997, sample 93 901), within error to the crystallization age of the post-D_2 Snot Rocks monzogranite. So here are two contemporaneous granites, one interpreted as pre- to syn-D_2 and the other as post-D_2. Nelson (1997) rationalised this discrepancy by using the errors on the ages to argue that the Split Rock granodiorite must have intruded during the waning stages of D_2, and the Snot Rocks soon after the end of D_2.

Nelson's (1997) interpretation is not particularly satisfactory because it attempts to fit the results of dating into a flawed granite classification. There are other, equally valid alternative interpretations consistent with available information. One alternative is that the Snot Rocks monzogranite crystallization age does not represent emplacement age (assumption (d) above) and that solid granite moved vertically after crystallization driven by its buoyancy (diapirism), thereby causing bending of regional trends. In this case the time of folding is unconstrained by granite crystallization age. Another possibility is that the sequence was folded against a pre-existing granite buttress emplaced at approximately 2660 Ma. In this case both folding and sedimentation are younger than the granitic rocks, and like the Split Rock, the Snot Rocks monzogranite is not post-D_2 but either pre- or syn-D_2. This interpretation is considered here as more likely because it provides a straightforward explanation for the similar ages of the Snot Rocks and Split Rocks granites and is fully consistent with the findings of Krapez et al. (2000) that the Kurrawang Sequence and its folding is younger than 2655 Ma.

5.1. Summary

The timing of D_2 and D_3 as interpreted here is summarized in Fig. 2. It has been demonstrated that the Snot Rocks monzogranite does not constrain the minimum age of D_2. Rather, we suggest that the Snot Rocks and Split Rocks granitoids were intruded pre- or syn-D_2 and that their presence, and not their emplacement, caused the deflection of the Kurrawang Syncline during D_2. In view of the findings of Krapez et al. (2000), it is suggested that D_2 folding started after 2655 Ma, post-dating the end of the deposition of the Kalgoorlie Sequence, and possibly contemporaneous with but most likely post-dating the deposition of the Kurrawang Sequence.

There are no simple rules to assess the age of granites in the Norseman-Wiluna Belt based on structural relationships. Each granite body and its relationships to regional structures need to be understood individually. Having demonstrated that D_2 and D_3 most likely developed after 2655 Ma, and not before 2660 Ma as previously thought, it is now possible to reinterpret the timing of other events by working backwards in time towards D_1.

6. Pre-D_2 extension phase: D_{2e}

Important subsidence before D_2 is required by the deep-marine nature of the turbidites of the Kalgoorlie and Kurrawang Sequences. Although subsidence may not necessarily be associated with extension, there is evidence for a phase of extension preceding D_2. This phase is here termed D_{2e} and it is suggested that early granite doming could have occurred during this phase.

6.1. Eastern Granitic Gneiss Complex

In this gneiss complex Swager and Nelson (1997) determined that the Barret Well granite gneiss and the foliated Two Lids Soak granodiorite crystallized at approximately 2675 Ma. These foliated rocks are intruded by massive monzogranite plutons that cross-cut regional structures, such as the normal Pinjin Fault. Small sheets of monzogranite are also present along the fault plane. These are foliated and contain the same steep north-plunging mineral lineation with west-block down kinematic indicators as found along the fault. The Pinjin fault is interpreted as an extensional feature which accommodated the uplift of gneiss and monzogranite but is also intruded by the monzogranite magma (Swager and Nelson, 1997). This younger monzogranite phase is presumed to be contemporaneous with the 2660 Ma intrusions of the Eastern Goldfields, and its deformation indicate that 'some uplift, accommodated by normal fault movement, occurred during intrusion' (Swager and Nelson, 1997). Because of the weak or absent foliation in the voluminous monzogranite plutons and their cross-cutting of the Pinjin Fault, the authors concluded that monzogranite intrusion at 2660 Ma dates the last stage of uplift of the granitic gneiss complex into the lower grade greenstone.

According to Swager and Nelson (1997), the evolution of the gneiss complex is characterized by three steps. The first step, deformation of the 2675 Ma gneisses occurred soon after their emplacement during D_1. The uplift of this high-grade gneissic complex postdates early D_1 and was accompanied and/or followed by intrusion of the monzogranite. Because the 2660 Ma age assigned to the massive monzogranite coincides with the established perception of the timing of D_2 shortening, the authors argue that doming took place in two further steps. First, an early dome developed during an extensional phase after D_1, then this was further uplifted during D_2 shortening and possibly driven by monzogranite intrusion, representing extensional structures developed during a shortening event.

The younger timing for D_2 deduced here (2655 Ma) implies that the 2660 Ma granites were not contemporaneous to shortening and that doming accompanied by monzogranite intrusion may have taken place during a single extensional phase, before D_2 shortening. Thus, rather than representing extensional structures during a shortening event, the Eastern Gneiss Complex is part of an extensional phase pre-dating D_2 shortening.

7. D_1 and D_{1e}

Moving further back in time, Krapez et al. (2000) constrained the unconformity marking the end of the Spargoville Sequence deposition and the start of the Kalgoorlie Sequence, to between 2683 and 2681 Ma based on zircon populations. This unconformity most likely represents an intrabasinal uplift (Krapez, personal communication 2000). It coincides temporally with the early intrusion of granites in the Norseman-Wiluna Belt, between 2685–2675 Ma ago (Nelson, 1997), as well as layered gabbro sills in the Kalgoorlie area (Mount Pleasant sill, *U–Pb* age 2687 ± 5 Ma, Kent and McDougall, 1995; Golden Mile Dolerite, 2675 ± 2 Ma, Bateman et al., 2001a). These early granites mark a change from predominantly extrusive magmatism to an extrusive-intrusive magmatic event. Time constraints on D_1 suggest that it was active after 2684 Ma (thrusting of the Bulong Anticline; Swager, 1997), during or soon after the emplacement of the approximately 2675 Ma Eastern Granitic Gneiss Complex (Fig. 2; Swager and Nelson, 1997) and before or during the intrusion of the 2674 ± 4 Ma felsic porphyry dyke, which crosscuts D_1 folds at Kalgoorlie (*U–Pb* age; Kent and McDougall, 1995).

It was argued here that a subsidence phase, possibly associated with extension, D_{2e}, must have been active during deposition of the younger part of the Kalgoorlie Sequence and early Kurrawang Sequence. However, it is also known that D_1 must have been active during the deposition of the early part of the Kalgoorlie Sequence since the sequence is deformed and repeated by D_1 thrusts (Fig. 2; Archibald et al., 1981). Based on these independent constraints, it is here proposed that the beginning of D_1 is marked by the initiation of plutonism at approximately 2685 Ma, and by the unconformity between the Spargoville and Kalgoorlie Sequences. D_1 was active during the deposition of the early part of the Kalgoorlie Sequence, which ended at approximately 2670 Ma, or alternatively there were two or more phases of D_1, bracketing the deposition of the early Kalgoorlie Sequence. This phase is responsible for early thrusting and possibly also nappe/slumping of the volcano-sedimentary sequence (Martyn, 1987; Passchier, 1994).

8. Numerical models of folding and rigid bodies

The close relationship between granites and regional folds warrants a more detailed study of the interaction between rigid-body granites and folding. Numerical models were designed to determine the role of pre-existing rigid bodies on folding of purely viscous, layered sequences. The Eastern Goldfields gross regional geology and seismic reflection profile reveals the geometry of antiforms cored by granites. Both pre- to syn-D_2 or post-D_2, granites have similar geometry (Swager et al., 1997; Swager, 1997). They are imaged seismically as approximately rectangular massive bodies with vertical eastern and western margins, truncating gently dipping fold limbs, and a flat bottom below which greenstones are continuous (Fig. 3a).

The code used is detailed in Moresi et al. (2001). The numerical models used a rectangular rigid body, analogue to the competent pluton, embedded in a horizontal layered sequence. The sequence was shortened by moving the right-hand side vertical wall (Fig. 3b). The model box width was three times its height. The layer embedding the 'granite' is overlain by material analogue to air (compressive and inviscid) and occupies initially half the height of the box. The 'granite' is embedded in a layer 100 times less viscous. This layer is underlain by a low viscosity layer at the base of the box (1000 times less viscous than the granite analogue). The narrow sub-layers in the embedding layer are competent, having the same viscosity as the granite.

The role of a rigid 'granite' during shortening is depicted in Fig. 4. The 'granite' was first modelled as having the same density as the country rocks (Fig. 4b), and made buoyant in a later model (Fig. 4c). The pattern of folding caused by the presence of the two narrow competent layers alone is shown in Fig. 4a. Fold wavelength is controlled by the width and viscosity contrast of the folding layers. (In the absence of the two narrow competent layers, layer shortening occurred without folding).

A rigid rectangle was introduced in Fig. 4b, in the position where the antiform formed in Fig. 4a. The rigid body, by inhibiting thickening of the embedding layer, triggered the downwarping of the layer to form a synform where there was previously an antiform. Antiforms developed where the layer thickened, away from the granite. Fig. 4c depicts the results where the rigid body was buoyant. In this example, the 'granite' forms the core of an antiform because its buoyancy was sufficiently important to overpower the tendency to downwarp the sequence into a synform. Folds in Fig. 4a attained the same amplitude as those in Fig. 4b and c only after considerably more shortening. This is because in the absence of the rigid 'granite' shortening could more easily be taken up by homogeneous layer thickening.

The development of the synform is not particularly sensitive to the shape and size of the granite body. Runs with a much narrower 'granite' (height of 0.05 instead of 0.24 in Fig. 4) resulted in similar folding as in Fig. 4b. However, when the granite is buoyant, whether a synform or an antiform develops depends on the ratio between rates of shortening and of doming. Faster shortening would inhibit doming and give rise to a granite-cored synform.

8.1. Summary and implications

The results indicate that rigid granitic bodies may trigger either growth of a synform or an antiform depending on the relative rates of shortening and buoyancy-driven doming. In nature, the presence of pre-deformation rigid plutons in the cores of antiforms indicates that their buoyancy may have played an active part during folding. This final geometry is, however, not unique as it would result also from the syn-tectonic emplace-

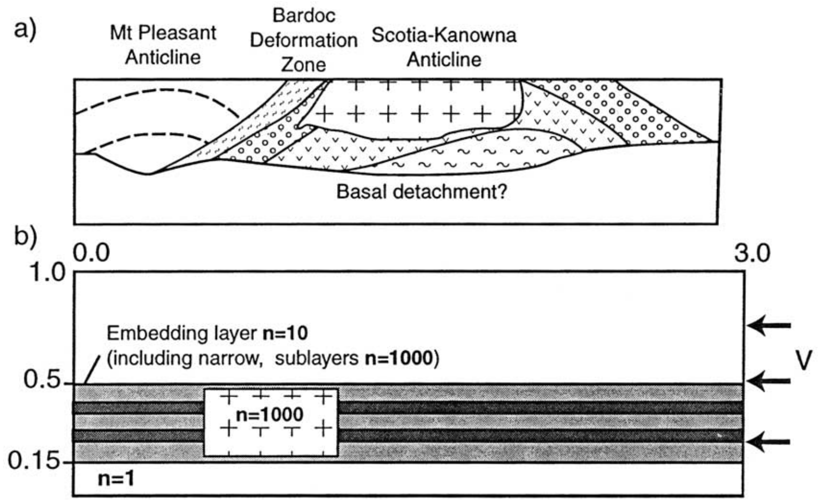

Fig. 3. (a) Seismic interpretation of the shape of a granite pluton and relation to country rocks in the Norseman-Wiluna Belt (after Swager et al., 1997, Fig. 10); (b) initial geometry and set-up of the numerical models. The model box has three wide layers: the bottom layer (viscosity $n = 1$), the middle layer ($n = 10$ and 1000), which embeds the rigid granite analogue (high viscosity rectangle, $n = 1000$), and the top layer corresponding to air.

ment and solidification of a buoyant magma body into the core of a developing antiform. It could be that in the same orogen, low buoyancy solid granitic bodies determine the sites of synformal folding, whereas large buoyancy bodies determine the sites of antiformal folding. The inverse is true for a low viscosity, dense, mass of ultramafic rock relatively localized (as opposed to an extensive, narrow layer): its low viscosity will speed up local layer shortening and antiform growth, whereas its high-density may lead to the sinking of the region into a synform.

9. Discussion

The revised timing of events in the Norseman-Wiluna Belt is summarized in Fig. 2. As noted by Davis and Forde (1994) the effects of metamorphic grade, deformation partitioning, diachroneity of deformation, successive deformations with common far-field stress directions, and the influence of pre-existing tectonic elements in the development of later ones, presents a formidable list of factors that must be considered when attempting to resolve the structural history of the belt. Here, only a few of these effects have been considered, and some, like diachroneity of deformation, have been left out of the discussion due to lack of information.

There are a number of observations which suggest that D_1 was active at around 2675 Ma, and that it has deformed at least part of the Kalgoorlie Sequence. In Fig. 2 the unconformity between the Spargoville and Kalgoorlie Sequences and the initiation of voluminous plutonic magmatism are ascribed tentatively to the onset of D_1. This was followed by a period of extension, D_{2e}, the pre-D_2 extensional phase of Witt (1994) and Swager (1997). This phase is related to the subsidence related to the deposition of the late stage of the Kalgoorlie Sequence and the subsequent deep-marine deposition of the Kurrawang Sequence.

Extension also accounts for doming at the Eastern Gneiss Complex and could arguably account for the extensional structures around Leonora (Williams and Currie, 1993; Williams

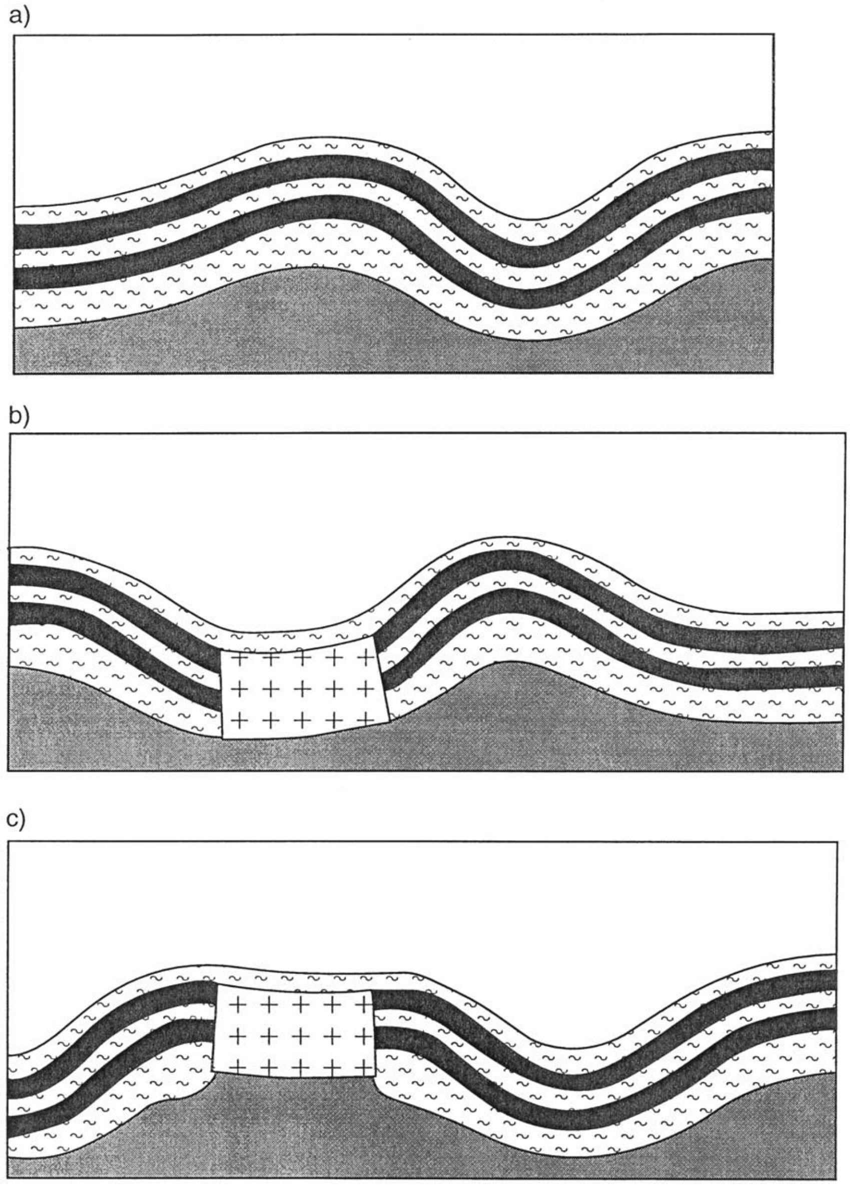

Fig. 4. Numerical models of folds developed in a layered sequence similar to Fig. 3. (a) Folding of simple layers; (b) 'granite pluton' (rectangle) was placed at the position where the anticline developed in (a), and caused synclinal folding. In this case all materials have the same density. (c) Same as (b) with the 'granite' being less dense than the surrounding. Whereas in (b) the rigid rectangle triggered synclinal folding, buoyancy in (c) led to anticlinal folding. In this case, if shortening rate is increased, the tendency of the rigid 'granite' to trigger synclinal folding will dominate.

and Whitaker, 1993), although Passchier (1994) suggested that extension could be either immediately before or contemporaneous with D_1 shortening in the Kalgoorlie area. Folding experiments described above indicate also that doming is not limited to extensional phases, and that buoyant granites could trigger the developments of doming antiforms during shortening phases. It is possible that granite doming occurred throughout the evolution of the belt.

The unconformity between the Kalgoorlie and Kurrawang Sequences is not accounted for by any major shortening event (Fig. 2) as it is unlikely that subsidence and deposition of a deep-marine succession would be contemporaneous with the crustal thickening event characterized by D_2. Furthermore, D_2 folded the <2655 Ma Kurrawang Sequence and must therefore have started either late during or after sedimentation of the Kurrawang Sequence. It is most likely that the unconformity between the Kalgoorlie and Kurrawang Sequence was a result of uplift and tilting related to changes in the extension regime, or some form of passive regional uplift.

Although the timing of D_2 is based on the late deposition of the Kurrawang Sequence determined by Krapez et al. (2000), the argument for a late D_2, at least younger than 2660 Ma, stands independently. The argument is based on the contemporaneous intrusion of the approximately 2660 Ma Snot and Split Rocks (see above), and their role in deflecting the regional trend of the D_2 Kurrawang Syncline, implying that these granites were already emplaced during folding.

The main conclusion reached here is that the bulk of deformation in the Norseman-Wiluna Belt (D_2–D_4) took place between 2650 and 2630 Ma. This is broadly contemporaneous with gold mineralisation and post-dates the main phase of granite intrusion.

10. Gold mineralisation, metamorphism and magmatism

10.1. Gold mineralisation

Age constraints of structurally controlled lode gold deposits in the Yilgarn Craton have recently been summarized by Yeats et al. (1999) and Groves et al. (2000). Timing of mineralisation is generally regarded as late in the tectonic evolution of the granitoid-greenstone terrains, during D_3 or D_4 (Mueller et al., 1988; Vearncombe et al., 1989; Clout et al., 1990; Groves et al., 1990; Groves et al. 2000; Ridley and Mengler, 2000), with a few important examples where mineralisation took place during D_2 like the Oroya Shoot at Kalgoorlie (e.g. Knight et al., 2000; Bateman et al., 2001b) or even possibly before the main D_2 phase, like the Golden Mile at Kalgoorlie (Bateman et al., 2001b; Fig. 2).

Groves et al. (2000) summarized the view held by several authors, that there has been a late Yilgarn-wide, gold mineralisation event, between about 2660 and 2610 Ma with most voluminous and widespread deposition between 2640 and 2630 Ma at the waning stages of the D_2–D_4 cycle (Fig. 2). During this event, metamorphic conditions remained very close to those recorded by peak mineral assemblages (McNaughton et al., 1990; Groves et al., 2000; Knight et al., 2000) so that gold-related wall-rock alteration assemblages vary systematically with metamorphic grade, with high-temperature alteration and metamorphic assemblages occurring around granitoids (Witt, 1991).

10.2. Metamorphism

Bickle and Archibald (1984) studied the metamorphic reactions of a sample collected 2 km away from the Widgiemooltha Dome. The sample records a temperature 530–560 °C at ~4 kbar. These conditions represent peak regional metamorphic conditions, independent from granite intrusion, and broadly coincide with regional conditions determined further north, near Coolgardie (Knight et al., 2000). Bickle and Archibald (1984) studied the reactions of another sample collected 700 m away from the margin of the Pioneer Dome. The sample records nearly isobaric heating from the regional conditions (560 °C at 4 kbar), to 600–650 °C. The high peak temperatures attained close to the granite are demonstrably related to granite magma emplacement and lead Bickle and Archibald (1984) to conclude that D_2–D_3 must have occurred soon after granite emplacement. However, the authors do not describe the relationship between metamorphic minerals and structures, making it impossible to critically analyse this conclusion.

Mueller and McNaughton (2000) discussed in detail metamorphism in the Southern Cross area (west of the Norseman-Wiluna Belt), and concluded that gold deposition did not occur during peak metamorphism, as previously thought, but 150 Ma later, at approximately 2620 Ma. They suggested that granite-centred metamorphic aureoles are related to granite magma emplacement, but due to different granite ages and the multi-pulse nature of some domes, peak temperatures in different aureoles were reached at different times, or developed over a long period, as a result of several thermal pulses. Mueller and McNaughton (2000) discussed the difficulties in deriving the relative timing between gold mineralisation and peak metamorphism from field and petrographic relationships. These results suggest caution when equating the age of individual high-temperature gold mineralisation to that of neighbouring granite intrusions (e.g. Witt, 1991; Knight et al., 2000).

Bickle and Archibald (1984) and Mueller and McNaughton (2000) showed how peak temperatures in granite aureoles are related to granite intrusions, temperature conditions away from granite margins are controlled by other heat sources such as heat flux from the mantle, crustal heat production and magma migration. The long magmatic and tectonic history of both the Southern Cross area and the Norseman-Wiluna Belt suggests that temperatures fluctuated over time, producing long-lasting and fluctuating low-pressure high-temperature conditions throughout the middle and upper crust. There are currently few age determinations of the timing of regional metamorphic peak. The prevalent view that voluminous granite magmatism at 2660 Ma is responsible for regional metamorphism must be proven rather than assumed, since it disregards other effects influencing the thermal history of the crust, such as crustal extension and shortening, and burial and exhumation of heat producing rocks.

Although high-temperature (>600 °C), narrow aureoles at the margins of granite domes are most likely related to magma cooling, wider and lower temperature contact aureoles may have alternative origins. One possibility is differential vertical uplift centred at buoyant granites and exhuming deeper and hotter rocks. Bickle and Archibald (1984) concluded that this was probably not the case for the Pioneer and Widgiemooltha Domes (isobaric heating), but this could nevertheless be the case for other domes across the belt. Another possibility is that high-temperatures result from fluid flow and heat advection along the strained granite margins. A final possibility is that the aureole results from a combination of higher granite conductivity and heat production, compared to greenstones. As illustrated by the Sybella Batholith in Mount Isa (Sandiford and Hand, 1998; McLaren et al., 1999), a granite body a few kilometers deep with high production and blanketed by low conductivity rocks may be a long-term heat source capable of imposing considerable long-term temperature perturbation on their surrounding.

Calculations using the values of conductivity for greenstones and quartz-porphyry (assumed to be similar to that of granites) measured in Norseman (Howard and Sass, 1964), and the average content of heat producing elements of the Bali Suite (granites near Coolgardie; Witt and Davy, 1997), indicate that the long-term horizontal thermal gradient around granites of vertical thickness of a few kilometers, is relatively weak (20–30 °C decay over 35 km) and can not account for an observable thermal aureole (Mike Sandiford, personal communication 2000). For the calculations, the average values used were $U = 4$ ppm, $Th = 22$ ppm and $K_2O = 4.2\%$ taken from Witt and Davy (1997) for the Bali Suite and exclude one anomalously high U sample. This suite includes several granites emplaced in a zone of amphibolite facies metamorphism around Coolgardie, including the Widgiemooltha granite. Heat production of Bali Suite granites would have been a reasonably high 5–6 $\mu W/m^3$ at 2.7 Ga, approximately double the heat production at present time. Low mantle heat flux into the base of the crust was used in the calculation.

These calculations suggest that a large proportion of the temperature difference between rocks near Coolgardie and rocks near Kalgoorlie (250–300 °C and ~ 2 kbar difference) is related to the different burial depths and regional vertical geothermal gradient and not to horizontal gradients imposed by different rates of heat production.

It is important, however, to point out that even a relatively small long-term, long-distance lateral temperature difference could be an important factor in controlling horizontal hydrothermal flow across the belt.

Thus, it seems unlikely that aureoles in the Norseman-Wiluna Belt result from granite radioactive heat production and high conductivity, supporting the view held by several authors that the granite-centred isograds results from magma intrusion (e.g. Witt, 1991). However, the other two possibilities to explain the aureoles (heat advection by fluid flow or differential exhumation around domes) remain viable alternatives.

At present there is insufficient reliable information to understand the pattern and timing of peak metamorphism across the belt. There are difficulties in establishing the timing of metamorphism in relation to deformation phases and gold deposition, and there are few reliable ages of peak metamorphism in the Norseman-Wiluna Belt. It is clear, however, that granite intrusion produces a narrow high-temperature arueole in its surroundings. Because of the variety of granite ages the aureoles are diachronous across the belt. There are other processes that could give rise to the wider, lower temperature contact aureole, although calculations suggest that horizontal thermal gradient caused by heterogeneous distribution of heat producing elements and conductivity differences may be neglected. Timing of peak metamorphism away from the very high-temperature aureoles ($>$ 600 °C) cannot be equated with the time of most voluminous magmatism, since it depends on the entire tectonothermal evolution of the belt.

10.3. Magmatism and deformation

Figure 5 summarizes the relationship between magma intrusion and deformation phase. Early granites ($>$2672 Ma) were intruded during shortening associated with D_1, as demonstrated by Swager and Nelson (1997). Different from previous authors, Krapez et al. (2000) suggested that the most voluminous intrusive phase (high-Ca), comprising plutons crystallized between 2670 and 2655 Ma, were emplaced during D_{2e} extension. Relatively small volumes of 2650–2630 Ma low-Ca granites and alkaline granites are exposed (Smithies and Champion, 1999) and were intruded during the D_2–D_4 deformation cycle. The alkaline granites have an A-type affinity, but as pointed out by these authors, their anorogenic tectonic setting cannot be inferred from their chemistry.

The Clarke Well granite, emplaced within rocks deformed by the Ida Fault zone, is only weakly deformed. If it can be assumed that its deformation is related to the waning stages of regional deformation (Nelson, 1997), an improvement of the error bar on its 2640 ± 8 Ma zircon (magma crystallization) age is required, since the present error bar covers most of the duration of the D_2–D_4 deformation cycle (Fig. 2).

The conclusion that the voluminous granite intrusions are pre-D_3, the transcurrent phase of deformation, is borne out also by the general shape of granite bodies throughout the belt. Even though shapes alone can not be used as indicators of timing in relation to deformation, the typically elliptical or spherical shape of plutons of the Norseman-Wiluna Belt (Witt and Swager, 1989; see also maps in Hallberg, 1986; Hammond and Nisbet, 1992; Williams and Whitaker, 1993; Swager and Nelson, 1997; Witt and Davy, 1997), are in stark contrast to shapes of granites intruded during transcurrent deformation. These are typically moulded by active shear zones: plutons may grow within the shear zone as a complex of sheared sheets (Main Donegal granite; Hutton, 1982); they may link two or more shear zones and exhibit magmatic foliation related to regional shearing (e.g. the Mortagne pluton, Britanny, Guineberteau et al., 1987; and plutons of the Borborema Province, Brazil, Neves at al., 1996; Jardim de Sá et al., 1999); or more characteristically, they may form elliptical plutons with sheared tails within shear zones (Fig. 6; the Ardara pluton, Pitcher and Berger, 1972; plutons of the Borborema Province, Neves et al., 1996; Jardim de Sá et al., 1999).

11. The Kalgoorlie orogen

Smithies and Champion (1999) defined three tectonothermal events in the Eastern Goldfields.

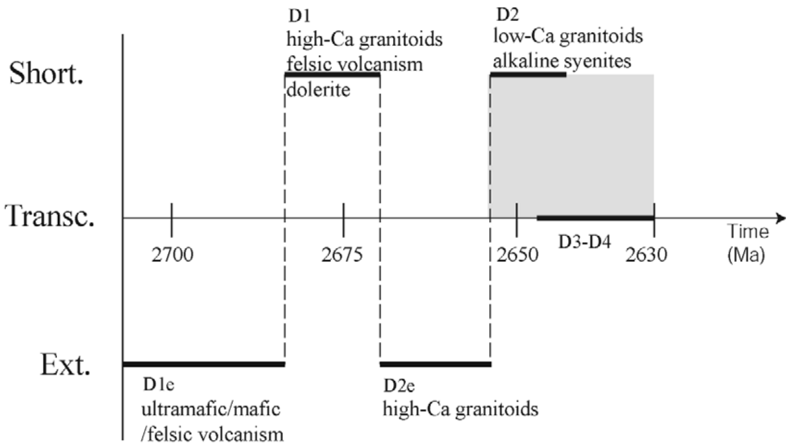

Fig. 5. Summarizing plot of the relationship between magmatism and inferred phase of deformation.

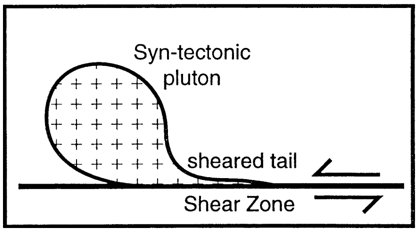

Fig. 6. Typical syn-tectonic pluton shape in transcurrent terranes.

The first one was marked by a major thermal anomaly at approximately 2705 Ma and the extrusion of komatiites and felsic volcanic rocks. The second event was marked by the main phase of regional magmatism, which according to them, started at approximately 2690 and peaked between 2670 and 2655 Ma. The third event spans the period between approximately 2650 and 2630 Ma, and is characterized by the intrusion of low-Ca granites and alkaline granites, and gold mineralisation. Smithies and Champion (1999) argued, based on Kent et al. (1996), Qiu (1997) and Ridley (1993), that despite small exposures, these late granites may be voluminous at depth, as observed in more deeply eroded terranes of the Yilgarn Craton (e.g. Southern Cross and Murchison Terranes). Kent et al. (1996) related gold mineralisation at 2640–2620 Ma and this late felsic magmatism to a period of lower-middle crustal reworking between 2650 and 2630 Ma, involving anatexis and granulite to amphibolite facies metamorphism (Ridley, 1993).

This work changes the character of the third tectonothermal event proposed by Smithies and Champion (1999). Rather than being characterized by extension and possibly driven by lithospheric delamination (Smithies and Champion, 1999), this event is characterized by a shortening cycle (D_2–D_4) and define an orogeny referred to here as the Kalgoorlie orogen. Gold mineralisation may have taken place above contemporaneous and voluminous magma intrusion at depth. The requirement of higher temperatures to produce A-type magmas ($\sim$850–950 °C; Clemens et al., 1986) indicates that temperatures underneath the Norseman-Wiluna Belt may have risen after the end of the earlier and voluminous I-type high-Ca magmatic event (Smithies and Champion, 1999). This could be a result of crustal thickening during D_2 thrusting and folding combined with the previous extraction of I-type melts, leaving a restitic lower crust (Clemens et al., 1986).

12. Conclusions

The new time constraints provided by the work of Krapez et al. (2000) and the scrutiny of implicit and explicit assumptions underlying earlier interpretations, have provided the basis for reinterpreting the timing of structural events in the Norseman-Wiluna Belt and for producing a self-consistent time chart. The main conclusions of this work are:

a) The onset of voluminous plutonism at approximately 2685 Ma, marks the onset of D_1 shortening after a period dominated by extension associated with mafic-ultramafic and felsic volcanism (D_{1e}). This change accounts for the unconformity between the Spargoville and the Kalgoorlie (Black Flag) Sequences (Krapez et al., 2000).
b) D_{2e} is an extensional event contemporaneous to subsidence and deposition of the late stage of the Kalgoorlie Sequence as well as the Kurrawang Sequence.
c) Doming of low-density granite masses may have occurred during D_{1e} (the Raeside Batholith; Williams and Whitaker, 1993; Passchier, 1994) or D_{2e} (the Eastern Gneiss Complex). Doming may also have occurred during shortening phases driven by granite buoyancy.
d) Buoyant competent granite bodies may trigger the nucleation and growth of antiforms. When buoyancy is negligible, the competent body will trigger nucleation of a synform.
e) D_2 is younger than previously thought (2655 Ma) and the D_2–D_4 deformation cycle took place between approximately 2650–2630 Ma, after the voluminous 2680–2685 Ma granitoid intrusion event.
f) D_2–D_4 crustal shortening cycle and the intrusion of less voluminous low-Ca and alkaline granitoids between 2650 and 2685 Ma define the Kalgoorlie orogen and is associated with gold mineralization. This conclusion contrasts with the previous suggestion that this late magmatic event was related with extension and possibly lithospheric delamination (Smithies and Champion, 1999).

The new time chart proposed here is consistent with the timing of sedimentation, as well as structural and magmatic events.

Acknowledgements

We would like to thank the discussion and helpful comments by Roger Bateman, Brett Davis, David Groves, Lyal Harris and Bryan Krapez, which much improved the ideas expressed in this paper. We also acknowledge Cees Swager and an anonymous reviewer for comments which much improved the manuscript.

References

Allibone, A.H., Norris, R.J., 1992. Segregation of leucogranite microplutons during syn-anatectic deformation: an example from the Taylor Valley. Antarctica J. Metam. Geol. 10, 589–600.

Archibald, N.J., Bettenay, L.F., 1977. Indirect evidence for tectonic reactivation of a pre-greenstone sialic basement in Western Australia. Earth Planet Sci. Lett. 33, 370–378.

Archibald, N.J., Bettenay, L.F., Bickle, M.J., Groves, D.I., 1981. Evolution of the Archaean crust in the Eastern Goldfields Province of the Yilgarn Block, Western Australia. Geol. Soc. Aust. Spec. Publ. 7, 491–504.

Archibald, N.J., Bettenay, L.F., Binns, R.A., Groves, D.I., Gunthorpe, R.J., 1978. The evolution of Archaean greenstone terrains, Eastern Goldfields Province, Western Australia. Precambrian Res. 6, 103–131.

Barley, M.E., Eisenlohr, B.N., Groves, D.I., Perring, C.S., Vearncombe, J.R., 1989. Late Archean convergent margin tectonics and gold mineralization: a new look at the Norseman-Wiluna Belt, Western Australia. Geology 17, 826–829.

Bateman, R., Costa, S., Swe, T., Lambert, D., 2001a. Archaean mafic magmatism in the Kalgoorlie area of the Yilgarn Craton, Western Australia: a geochemical and Nd isotopic study of the petrogenetic and tectonic evolution of a greenstone belt. Precambrian Res. 108, 75–112.

Bateman, R.J., Hageman, S.G., McCuaig, T.C., Swager, C.P., 2001b. Protracted gold mineralization throughout Archaean orogenesis in the Kalgoorlie camp, Yilgarn Craton, Western Australia: structural, mineralogical, and geochemical evolution. In: World-Class Gold Camps and Deposits in the Eastern Yilgarn Craton, Western Australia, with Special Emphasis on the Eastern Goldfields Province, Hagemann, S.G., Neumayr, P., Witt, W.K., (Eds.). Western Australia Geological Survey, Record 2001/17, pp. 63–98.

Bickle, M.J., Archibald, N.J., 1984. Chloritoid and staurolite stability: implications for metamorphism in the Archaean Yilgarn Block, Western Australia. J. Metam. Geol. 2, 179–203.

Brown, S.J.A., Krapez, B., Beresford, S.W., Cassidy, K.F., Champion, D.C., Barley, M.E., Cas, R.A.F., 2001. Archaean volcanic and sedimentary environments of the

Eastern Goldfields Province, Western Australia—a field guide. Geol. Surv. Western Australia. Record. 2001/13, 66.

Campbell, I.H., Hill, R.I., 1988. A two-stage model for the formation of the granite-greenstone terrains of the Kalgoorlie-Norseman area, Western Australia. Earth Planet Sci. Lett. 90, 11–25.

Champion, D.C., Sheraton, J.W., 1997. Geochemistry and Nd isotope systematics of Archaean granites of the Eastern Goldfields, Yilgarn Craton, Australia: implications for crustal growth processes. Precambrian Res. 83, 109–132.

Clemens, J.D., Holloway, J.R., White, A.J.R., 1986. Origin of an A-type granite: experimental constraints. Am. Miner. 71, 317–324.

Clout, J.M.F., Cleghorn, J.H., Eaton, P.C., 1990. Geology of the Kalgoorlie gold field. In: Hughes, F.E. (Ed.), Geology of the Mineral Deposits of Australia and Papua New Guinea. The Australasian Institute of Mining and Metallurgy, Parkville, Australia, pp. 411–431.

Davis, B.K., 1993. Mechanism of emplacement of the Cannibal Creek Granite with special reference to timing and deformation history of the aureole. Tectonophysics 224, 337–362.

Davis, B.K., Forde, A., 1994. Regional slaty cleavage formation and fold axis rotation by re-use and reactivation of pre-existing foliations; the Fiery Creek slate belt, North Queensland. Tectonophysics 230, 161–179.

Davis, B.K., Pollard, P.J., Lally, J.H., McNaughton, N.J., Blake, K., Williams, P.J., 2001. Deformation history of the Naraku Batholith, Mt Isa Inlier, Australia: implications for pluton ages and geometries from structural study of the Dipvale granodiorite and Levian granite. Aust. J. Earth Sci. 48, 113–129.

Drummond, B.J., Goleby, B.R., Swager, C.P., Williams, P.R., 1993. Constraints on Archaean crustal composition and structure provided by deep seismic sounding in the Yilgarn Block. Ore. Geol. Rev. 8, 17–24.

Gee, R.D., 1979. Structure and tectonic style of the Western Australia Shield. Tectonophysics 58, 327–369.

Goleby, B.R., Rattenbury, M.S., Swager, C.P., Drummond, B.J., Williams, P.R., Sheraton, J.W., Heinrich, C.A., 1993. Archaean crustal structure from seismic reflection profiling, Eastern Goldfields, Western Australia. Austr. Geol. Surv. Org. Rec. 15, 54.

Groves, D.I., Batt, W.D., 1984. Spatial and temporal variations in Archaean metallogenic associations in terms of evolution of granitoid-greenstone terrains with particular emphasis on the Western Australian Shield. In: Kröner, A., Hanson, G.N., Goodwin, A.M. (Eds.), Archaean Geochemistry: The Origin and Evolution of the Archaean Continental Crust. Springer-Verlag, Berlin, pp. 73–98.

Groves, D.I., Knox-Robinson, C.M., Ho, S.E., Rock, N.M.S., 1990. An overview of Archaean lode-gold deposits. In: Ho, S.E., Groves, D.I., Bennett, J.M. (Eds.), Gold Deposits of the Yilgarn Block, Western Australia: Nature, Genesis and Exploration Guides. Department of Geology and University Extension, University of Western Australia Publication, Perth, pp. 1–18.

Groves, D.I., Ridley, J.R., Bloem, E.M.J., Gebre-Mariam, M., Hageman, S., Hronsky, J.M.A., Knight, J.T., McNaughton, N.J., Ojala, J., Vielreicher, R.M., McGuaig, T.C., Holyland, P.N., 1995. Lode gold deposits of the Yilgarn block: products of late Archaean crustal-scale overpressured hydrothermal systems. Geological Society of London, Special Publications. Vol. 95, pp. 155–172.

Groves, D.I., Goldfarb, R.J., Knox-Robinson, C.M., Ojala, J., Gardoll, S., Yun, G.Y., Holyland, P., 2000. Late-kinematic timing of orogenic gold deposits and significance for computer based exploration techniques with emphasis on the Yilgarn Block, Western Australia. Ore. Geol. Rev. 17, 1–38.

Guineberteau, B., Bouchez, J.-L., Vigneresse, J.L., 1987. The Mortagne granite pluton (France) emplaced by pull-apart along a shear zone: structural and gravimetric arguments and regional implications. Bull. Geol. Soc. Am. 99, 763–770.

Hallberg, J.A., 1986. Archaean basin development and crustal extension in the northeastern Yilgarn Block, Western Australia. Precambrian Res. 31, 133–156.

Hammond, R.L., Nisbet, B.W., 1992. Towards a structural and tectonic framework for the central Norseman-Wiluna greenstone belt, Western Australia. In: Glover, J.E., Ho, S.E. (Eds.), The Archaean: Terrains, Processes and Metallogeny: Geology Department (Key Centre) and University Extension. University of Western Australia, Perth, pp. 39–50.

Howard, L.E., Sass, J.H., 1964. Terrestrial heat flow in Australia. J. Geophys. Res. 69, 1617–1626.

Hutton, D.H.W., 1982. A tectonic model for the emplacement of the Main Donegal granite, NW Ireland. J. Geol. Soc. Lond. 139, 615–631.

Jardim de Sá, E.F., Trindade, R.I.F., Hollanda, M.H.B.M., Araújo, J.M.M., Galindo, A.C., Amaro, V.E., Souza, Z.S., Vigneresse, J.-L., Lardeaux, J.-M., 1999. Brasiliano syntectonic alkaline granites emplaced in a strike slip/extensional setting (eastern Seridó, NE Brazil). An. Acad. Bras. Ci. 71, 17–27.

Kent, A.J.R., Cassidy, K.F., Fanning, C.M., 1996. Archean gold mineralization synchronous with the final stages of cratonization, Yilgran Craton, Western Australia. Geology 24, 879–882.

Kent, A.J.R., McDougall, I., 1995. 40Ar–39Ar and U–Pb age constraints on the timing of gold mineralization in the Kalgoorlie gold field, Western Australia. Econ. Geol. 90, 845–859.

Knight, J.T., Groves, D.I., Ridley, J.R., 1993. The Coolgardie Goldfield, Western Australia: district-scale controls on an Archaean gold camp in an amphibolite facies terrane. Miner. Deposita 28, 436–456.

Knight, J.R., Ridley, J.R., Groves, D.I., 2000. The Archean amphibolite facies Coolgardie goldfield, Yilgarn Craton, Western Australia: nature, controls, and fold field-scale patterns of hydrothermal wall-rock alteration. Econ. Geol. 95, 49–84.

Krapez, B., Brown, S.J.A., Hand, J., Barley, M.E., Cas, R.A.F., 2000. Age constraints on recycled crustal and supracrustal sources of Archaean metasedimentary sequences, Eastern Goldfields Province, Western Australia: evidence from SHRIMP zircon dating. Tectonphysics 322, 89–133.

Martyn, J.E., 1987. Evidence for structural repetition in the greenstones of the Kalgoorlie District, Western Australia. Precambrian Res. 37, 1–18.

McLaren, S., Sandiford, M., Hand, M., 1999. High radiogenic heat-producing granites and metamorphism—an example from the western Mount Isa inlier, Australia. Geology 27, 679–682.

McNaughton, N.J., Cassidy, K.F., Groves, D.I., Perring, C.S., 1990. Timing of mineralization. In: Ho, S.E., Groves, D.I., Bennett, J.M. (Eds.), Gold Deposits of the Yilgarn Block, Western Australia: Nature, Genesis and Exploration Guides. Department of Geology and University Extension. University of Western Australia Publication, Perth, pp. 221–225.

Moresi, L., Muhlhaus, H-B., Dufour, F., 2001. Particle-in-cell solutions for creeping viscous flows with internal interfaces. In: Muhlhaus, H-B., Dyskin, A., Pasternak, E. (Eds.), Proceedings of the Fifth International Workshop on Bifurcation and Localization in Geomechanics, Perth, WA., Australia: Balkema, Rotterdam, pp. 345–354.

Mueller, A.G., Harris, L.B., Lungan, A., 1988. Structural control of greenstone-hosted gold mineralization by transcurrent shearing: a new interpretation of the Kalgoorlie Mining District, Western Australia. Ore. Geol. Rev. 3, 359–387.

Mueller, A.G., McNaughton, N.J., 2000. U–Pb ages constraining batholith emplacement, contact metamorphism, and the formation of gold and W–Mo skarns in the Southern Cross area, Yilgarn Craton, Western Australia. Econ. Geol. 95, 1231–1257.

Nelson, D.R., 1997. Evolution of the Archaean granite-greenstone terranes of the Eastern Goldfields, Western Australia: SHRIMP U–Pb zircon constraints. Precambrian Geol. 83, 57–81.

Neves, S.P., Vauchez, A., Archanjo, C.J., 1996. Shear zone-controlled magma emplacement or magma-assisted nucleation of shear zones? Insights from northeast Brazil. Tectonophysics 262, 349–364.

Passchier, C.W., 1994. Structural geology across a proposed terrane boundary in the eastern Yilgarn craton, Western Australia. Precambrian Res. 68, 43–64.

Paterson, S.R., Tobisch, O.T., 1988. Using pluton ages to date regional deformation: problems with commonly used criteria. Geology 16, 1108–1111.

Pitcher, W.S., Berger, A.R., 1972. The geology of Donegal: a study of granite emplacement and unroofing: Regional Geology Series. Wiley, New York, p. 435.

Platt, J.P., Allchurch, P.D., Rutland, R.W.R., 1978. Archaean tectonics in the Agnew supracrustal belt, Western Australia. Precambrian Res. 7, 3–30.

Qiu, Y., 1997. Long-lived granitoid magmatism in the Southern Cross Province, Yilgarn Craton, Western Australia, and its relationships with Archaean lode-gold mineralization (unpublished Ph.D. thesis): University of Western Australia, 297 + appendix p.

Ridley, J., Implications of metamorphic patterns to tectonic models of the Eastern Goldfields. In: Williams, P.R., Haldane, J.A., (Compilers), Kalgoorlie 93—An International Conference on Crustal Evolution, Metallogeny and Exploration of the Eastern Goldfields. Australian Geological Survey Organization, pp. 95–100.

Ridley, J., Mengler, F., 2000. Lithological and structural controls on the form and setting of vein stockwork orebodies at the Mount Charlotte Gold Deposit, Kalgoorlie. Econ. Geol. 95, 85–98.

Robin, P.-Y., 1979. Theory of metamorphic segregation and related processes. Geochim. Cosmoch. Acta 43, 1587–1600.

Sandiford, M., Hand, M., 1998. Australian Proterozoic high-temperature, low-pressure metamorphism in the conductive limit. In: Treloar, P.J., O'Brien, P.J. (Eds.), What Drives Metamorphism and Metamorphic Reactions. Geology Society of London, Special Publication, Vol. 138, pp. 109–120.

Smithies, R.H., Champion, D.C., 1999. Late Archaean felsic alkaline igneous rocks in the Eastern Goldfields, Yilgarn Craton, Western Australia: a result of lower crustal delamination? J. Geol. Soc. Lond. 156, 561–576.

Swager, C., Griffin, T.J., 1990. An early thrust duplex in the Kalgoorlie–Kambalda greenstone belt, Eastern Goldfields Province, Western Australia. Precambrian Res. 48, 63–73.

Swager, C.P., 1997. Tectono-stratigraphy of late Archaean greenstone terranes in the southern Eastern Goldfields, Western Australia. Precambrian Res. 83, 11–42.

Swager, C.P., Goleby, B.R., Drummond, B.J., Rattenbury, M.S., Williams, P.R., 1997. Crustal structure of granite-greenstone terranes in the Eastern Goldfields, Yilgarn Craton, as revealed by seismic reflection profiling. Precambrian Res. 83, 43–56.

Swager, C.P., Nelson, D.R., 1997. Extensional emplacement of a high-grade granite gneiss complex into low-grade greenstones, Eastern Goldfields, Yilgarn Craton, Western Australia. Precambrian Res. 83, 203–219.

Swager, C.P., Witt, W.K., Griffin, T.J., Ahmat, A.L., Hunter, W.M., McGoldrick, P.J., Wyche, S., 1992. Late Archaean granite-greenstones of the Kalgoorlie Terrane, Yilgarn Craton, Western Australia. In: Glover, J.E., Ho, S.E. (Eds.), The Archaean: Terrains, Processes and Metallogeny: Geology Department (Key Centre) and University Extension. University of Western Australia, Perth, pp. 107–122.

Vearncombe, J.R., Barley, M.E., Eisenlohr, B.N., Groves, D.I., Houstoun, S.M., Skwarnecki, M.S., Grigson, M.W., Partington, G.A., 1989. Structural controls on mesothermal gold mineralization: examples from the Archean terranes of southern Africa and Western Australia. Econ. Geol. Monogr. 6, 124–134.

Weinberg, R.F., 1996. The ascent mechanism of felsic magmas: news and views. Trans. R. Soc. Edinburgh: Earth Sci. 87, 95–103.

Weinberg, R.F., Podladchikov, Y.Y., 1995. The rise of solid-state diapirs. J. Struct. Geol. 17, 1183–1195.

Williams, P.R., Currie, K.L., 1993. Character and regional implication of the sheared Archaean granite-greenstone contact near Leonora, Western Australia. Precambrian Res. 62, 343–365.

Williams, P.R., Whitaker, A.J., 1993. Gneiss dome and extensional deformation in the highly mineralised Archean Eastern Goldfields Provinces Western Australia. Ore. Geol. Rev. 8, 141–162.

Wintsch, R.P., Christoffersen, R., Kronenberg, A.K., 1995. Fluid-rock reaction weakening of fault zones. J. Geophys. Res. 100, 13021–13032.

Witt, N.K., Davy, R., 1997. Geology and geochemistry of Archaean granites in the Kalgoorlie region of the Eastern Goldfields, Western Australia: a syn-collisional tectonic setting? Precambrian Res. 83, 133–183.

Witt, W.K., 1991. Regional metamorphic controls on alteration associated with gold mineralization in the Eastern Goldfields Province, Western Australia: implications for the timing and origin of Archean lode-gold deposits. Geology 19, 982–985.

Witt, W.K., 1994. Geology of the Melita 1:100 000 Sheet, Explanatory Notes. Geological Survey of Western Australia 63.

Witt, W.K., Swager, C.P., 1989. Structural setting and geochemistry of Archaean I-type granites in the Bardoc-Coolgardie area of the Norseman-Wiluna Belt, Western Australia. Precambrian Res. 44, 323–351.

Yeats, C.J., McNaughton, N.J., Ruettger, D., Bateman, R., Groves, D.I., Harris, J.L., Kohler, E., 1999. Evidence for diachronous Archaean lode gold mineralization in the Yilgarn Craton, Western Australia: a SHRIMP U-Pb study of intrusive rocks. Econ. Geol. 94, 1259–1276.